

# Investigating hidden sectors at future $e^+e^-$ colliders through two-particle angular correlations

Emanuela Musumeci<sup>1,\*</sup>

<sup>1</sup>Instituto de Física Corpuscular (IFIC), CSIC – Universitat de València, C/ Catedrático José Beltrán 2, 46980 Paterna (Valencia), Spain

**Abstract.** Exploring long-range angular correlations among emitted particles in high-energy collisions provides an opportunity to uncover physics beyond the Standard Model like Hidden Valley (HV) models. We focus on a hidden QCD-like sector, where the interplay between HV matter and QCD partonic cascades could enhance azimuthal correlations between final-state particles. Our investigation, performed at detector level, specifically targets the detectability of these phenomena at future  $e^+e^-$  colliders, yielding a cleaner experimental signature as compared to the Large Hadron Collider (LHC). Remarkably, the observation of ridge structures in the two-particle correlation function may suggest the existence of New physics.

## 1 Introduction

This study investigates potential irregularities in azimuthal and rapidity correlations to explore the possible presence of New Physics beyond traditional QCD parton showers. Specifically, the focus is on two-particle angular correlations as indicators of beyond the Standard Model (BSM) physics at future high-energy  $e^+e^-$  colliders. In this analysis, the thrust reference frame is employed, thus rapidity  $y$  and azimuthal angle  $\phi$  are defined relative to this axis. The observables of interest are the rapidity and azimuthal differences,  $\Delta y$  and  $\Delta\phi$ , between two final-state charged particles. The *two-particle correlation function* is defined as:

$$C^{(2)}(\Delta y, \Delta\phi) = \frac{S(\Delta y, \Delta\phi)}{B(\Delta y, \Delta\phi)}, \quad (1)$$

where  $S(\Delta y, \Delta\phi)$  and  $B(\Delta y, \Delta\phi)$  are the same-event and mixed-event pair densities, respectively. Of particular interest is the azimuthal *Yield*  $Y(\Delta\phi)$ , defined by integrating over a range of rapidity differences:

$$Y(\Delta\phi) = \frac{\int_{y_{\text{inf}}}^{y_{\text{sup}}} S(\Delta y, \Delta\phi) d\Delta y}{\int_{y_{\text{inf}}}^{y_{\text{sup}}} B(\Delta y, \Delta\phi) d\Delta y}, \quad (2)$$

where the integration limits  $y_{\text{inf}}$  and  $y_{\text{sup}}$  specify the rapidity range of interest.

\*e-mail: emanuela.musumeci@ific.uv.es

## 2 Theoretical framework

The New Physics (NP) scenario considered in this study is the so-called Hidden Valley (HV). In many HV models, like those discussed in [1], the Standard Model (SM) gauge group  $G_{\text{SM}}$  is extended by introducing a new gauge group,  $G_V$ , under which a new class of particles, called *v-particles*, are charged, while remaining neutral under  $G_{\text{SM}}$ . Conversely, SM particles are neutral under  $G_V$ . To allow communication between the SM and HV sectors, additional particles known as *communicators* are introduced, which have charges under both  $G_{\text{SM}}$  and  $G_V$ . Communicators can be massive vector bosons, labeled as  $Z_v$ , or hidden partners of SM quarks and leptons, collectively called  $F_v$ . For this analysis,  $F_v$  is assumed to be the spin-1/2 fermionic mediator, while *v*-quarks from the Hidden Sector,  $q_v$ , are considered to be scalar particles.

The HV and SM sectors can interact through several processes. One possibility is a tree-level interaction such as  $e^+e^- \rightarrow Z_v \rightarrow q_v\bar{q}_v$ , leading to hadron production. Alternatively, communicators can be pair-produced through the SM  $\gamma^*/Z$  interaction, resulting in an  $F_v\bar{F}_v$  pair. This process gives rise to both visible and invisible cascades within the same event and this channel is found to dominate within the energy ranges of interest in our study.

In certain regions of the HV parameter space, communicators can decay rapidly into a visible SM particle ( $f$ ) and a hidden sector particle ( $q_v$ ), via the process  $F_v \rightarrow f q_v$ . The mass of  $q_v$  plays a significant role in determining the kinematics of the event, particularly in the visible cascade leading to SM final states. The mass of  $q_v$  is not yet constrained, ranging from close to zero to the mass of  $F_v$ . Different values of this mass are assumed in our analysis to explore its impact on observables.

This study focuses on how the presence of the hidden sector alters the behavior of partonic cascades producing final-state SM particles. Both visible and hidden cascades share the total event energy, which affects the phase space available to each sector. We consider a QCD-like HV scenario, where the hidden sector consists of  $q_v$ -quarks and  $g_v$ -gluons, with an effective strong coupling constant  $\alpha_v$ . For simplicity,  $\alpha_v$  is fixed at 0.1, as variations in this value do not significantly impact the results.

## 3 Detector-Level Analysis

To assess the detectability of the HV signal in  $e^+e^-$  collider environments, we utilized the PYTHIA [2] Monte Carlo event generator, which already includes HV production mechanisms. Fast detector simulations were conducted using the SGV package [3], with the detector geometry and acceptance based on the ILD [4] large model for the International Linear Collider (ILC) [5]. The simulation outputs followed the same event model as the ILD concept group and we used tools from ILCSOFT for event reconstruction. This reconstruction, based on the Particle Flow method, aims to identify all particles in the final state using pattern recognition algorithms, resulting in Particle Flow Objects (PFOs).

We focused our analysis at  $\sqrt{s} = 250$  GeV, coinciding with the first phase of ILC operation as a Higgs factory and further extended our study to higher energies up to 500 GeV and 1 TeV at particle level. Beam polarization effects will be investigated in future work.

The HV signal involves the process  $e^+e^- \rightarrow D_v\bar{D}_v \rightarrow \text{hadrons}$ , where  $D_v$  is the hidden sector partner of the  $d$ -quark. Our benchmark parameters include  $\alpha_v = 0.1$ ,  $m_{D_v} = 80, 100$  and 125 GeV, and various *v*-quark mass scenarios. Additional configurations and  $T_v\bar{T}_v$  production were considered at higher  $\sqrt{s}$ .

We present the HV signal and SM background cross-sections in Table 1, alongside the selection efficiencies. The selection cuts significantly reduce the background while maintaining a substantial fraction of the HV signal. In our analysis at  $\sqrt{s} = 250$  GeV, the primary back-

**Table 1.** Cross-sections for  $e^+e^- \rightarrow D_v\bar{D}_v$ ,  $e^+e^- \rightarrow q\bar{q}$  and  $WW \rightarrow 4q$  processes at  $\sqrt{s} = 250$  GeV, with different assignments for the  $m_{D_v}$  and  $m_{q_v}$  masses. Efficiencies of the selection criteria described in the main text, average charged-track multiplicities and their  $RMS$ , are shown.

Process		$\sigma_{\text{PYTHIA8}}$ [pb]	Efficiency [%]	$\langle N_{\text{ch}} \rangle$
$e^+e^- \rightarrow D_v\bar{D}_v$	$m_{D_v}$			
$m_{q_v} = 0.1$ GeV	125 GeV	0.13	36	$12.4 \pm 3.7$
$m_{q_v} = 10$ GeV	125 GeV	0.12	36	$12.4 \pm 3.7$
$m_{q_v} = 50$ GeV	125 GeV	0.12	42	$11.4 \pm 3.5$
$m_{q_v} = 100$ GeV	125 GeV	0.12	42	$6.5 \pm 2.1$
$m_{q_v} = 50$ GeV	100 GeV	1.29	42	$11.1 \pm 3.4$
$m_{q_v} = 40$ GeV	80 GeV	1.54	36	$18.0 \pm 4.9$
$e^+e^- \rightarrow q\bar{q}$ with ISR		48	$\lesssim 0.01$	$9.9 \pm 3.4$
$WW \rightarrow 4q$		7.4	$\lesssim 0.001$	–

ground originates from  $e^+e^- \rightarrow q\bar{q}$ , which includes all SM quark flavors except for the top quark, which production is below threshold.

In a previous study [6], the signal and background were investigated at particle level without including Initial State Radiation (ISR), though ISR plays a crucial role in this type of analysis, as will become clear. Four-fermion production, dominated by  $e^+e^- \rightarrow WW$ , was also excluded in that study. Here, we extend the analysis to detector level, now including the effects of ISR and  $e^+e^- \rightarrow WW \rightarrow 4q$ . The cross-sections for both HV and SM processes, as computed using PYTHIA, are shown in Table 1. Given the small cross-sections for HV production, specific cuts are necessary to reduce the background while preserving as much of the signal as possible. This analysis focuses on prompt decays of  $v$ -particles, excluding displaced vertices from long-lived particles, as we are primarily concerned with the prompt decays leading to SM final states.

Following a similar approach to Ref. [7], we impose constraints on the number of neutral and charged PFOs, with upper limits of 22 and 15, respectively. Additional cuts are applied to the ISR photon angle ( $|\cos \theta_{\gamma_{\text{ISR}}}| < 0.5$ ) and energy ( $E_{\gamma_{\text{ISR}}} < 40$  GeV), while the di-jet invariant mass  $m_{jj}$  is constrained to values below 130 GeV. The energy of the leading jet is further limited to 80 GeV. These selection cuts drastically reduce the SM background, as seen in Table 1, while having a smaller effect on the HV signal.

For the computation of  $B$  appearing in Eq. 1, we require a thrust value greater than 0.95, while maintaining the same constraints on PFO multiplicities as used for  $S$ .

To explore the potential for distinguishing HV signals from SM background, Fig. 1 presents the yield  $Y(\Delta\phi)$  (as defined in Eq. (2)) for the rapidity interval  $0 < |\Delta y| \leq 1.6$ , as it turns out to be particularly relevant. The yield is shown before and after cuts. Various HV signal masses  $m_{D_v}$  and  $m_{q_v}$  are compared with the SM background and a standalone SM analysis is also presented. In the range  $0 < |\Delta y| \leq 1.6$ , a prominent peak at  $\Delta\phi \sim \pi$  characterizes the HV case, while this feature is absent in the SM-only scenario. This clear difference in shape could serve as a useful signature of a hidden sector, providing a complementary approach to the conventional searches.

An outlook at higher energies ( $\sqrt{s} = 500$  GeV and 1 TeV) was conducted, as detailed in [8]. In this analysis, we investigate two extreme cases: the lightest communicator  $D_v$  and the heaviest  $T_v$ , which decays into  $q_v t$ . Our findings indicate that intermediate masses yield intermediate results. A part from the  $q\bar{q}$  and  $WW \rightarrow 4q$  backgrounds, we also take into

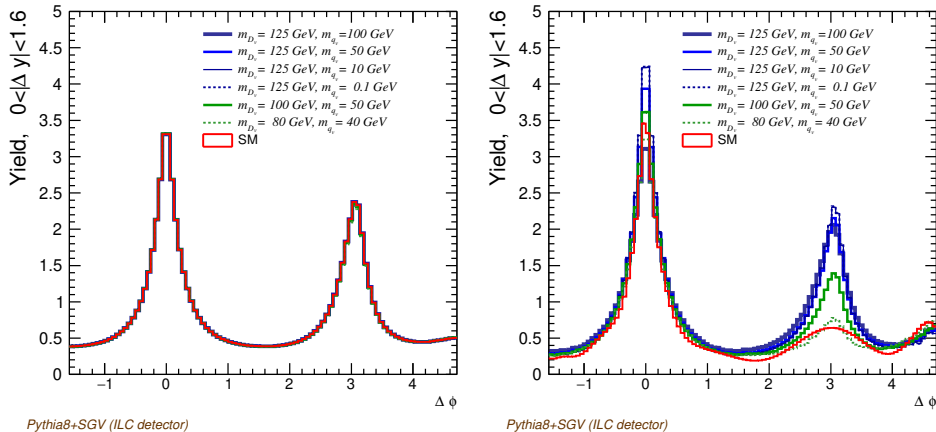


**Figure 1.** Yield  $Y(\Delta\phi)$  for both HV signal in association with SM and for pure SM background (red line) for the  $0 < |\Delta y| < 1.6$  before (left) and after cuts (right) .

account  $t\bar{t}$  production, which becomes increasingly relevant at these energies. We observed similarly encouraging prospects for the HV signal.

## 4 Prospects on the experimental sensitivity

A study assuming different scenarios for the foreseen statistical and systematic uncertainties was performed.

To estimate the statistical uncertainties, we assume a collected luminosity of  $100 \text{ fb}^{-1}$ , which roughly corresponds to one year of data taking of ILC in the H20-staged scenario [9]. We have identified two primary sources for the systematic uncertainties: the modelling of detector performance and uncertainties related to fragmentation, specifically the final hadronization process of the partonic cascade. Due to the current state of knowledge, our estimates for both sources are largely educated guesses.

For the detector performance modelling uncertainty, we evaluate it through a bin-by-bin comparison of yield distributions at the particle level and detector level, taking the absolute difference as the uncertainty. This analysis must consider kinematic resolution, including angular measurements, as well as acceptance effects. It is essential to emphasize that this method likely overestimates experimental uncertainties, representing a worst-case scenario.

In a similar fashion, for fragmentation uncertainty, we utilize a comparable methodology, comparing yield predictions at the particle level generated by two distinct fragmentation models implemented in PYTHIA and HERWIG [10, 11]. The overall uncertainty is calculated on a bin-by-bin basis, combining the statistical uncertainty for the anticipated number of events with the systematic uncertainties of  $Y_{SM}$  in quadrature, as only PYTHIA accounts for Hidden Valley production. The summary of these findings is presented in Fig. 2, with  $\sigma_Y$  denoting the estimated uncertainty as outlined.

Taking all the aforementioned points into consideration, calculating the sensitivity of the observable becomes straightforward by comparing the predictions of Hidden Valley (HV) and Standard Model (SM) for  $Y$  against the anticipated uncertainties. Even with a collected luminosity of  $100 \text{ fb}^{-1}$ , sensitivity is primarily constrained by systematic uncertainties, with the systematic errors associated with detector performance being the most significant. Neverthe-

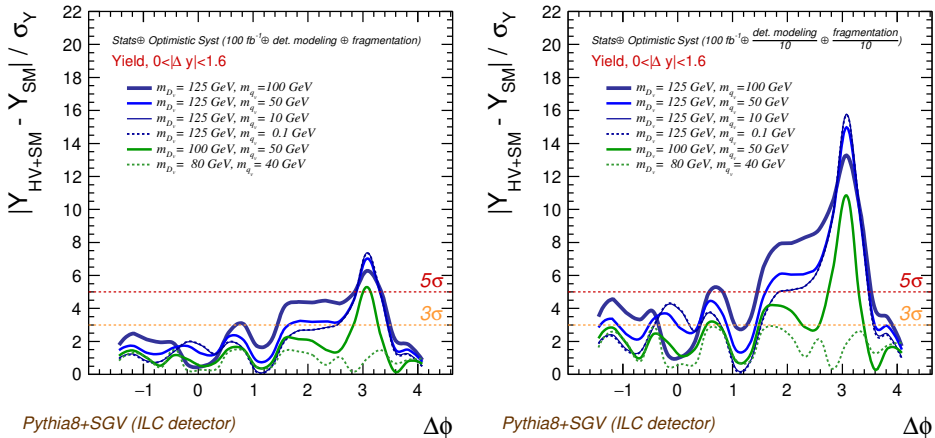


**Figure 2.** Expected experimental sensitivity for Hidden Valley models along with the SM background after collecting  $100 \text{ fb}^{-1}$  of integrated luminosity, for yield measurements in the range of  $0 < |\Delta y| < 1.6$ . With systematic modelling uncertainties obtained from current state of the art (left) and assuming an improvement of one order magnitude on the modelling uncertainties evaluation (right).

less, the discovery potential remains largely unaffected, particularly around the pronounced  $Y$  peak at  $\Delta\phi \sim \pi$  within the range of  $0 < |\Delta y| \leq 1.6$ .

To illustrate this, we compare the estimated sensitivity to a more optimistic scenario, wherein we enhance our understanding of systematic uncertainties by an order of magnitude relative to current estimates, assuming considerable advancements in detector performance-related uncertainties. Furthermore, dedicated investigations into the fragmentation modelling of HV processes would be essential for a deeper comprehension of these aspects. With such an improvement, we would expect a substantial increase in sensitivity, enabling the discovery potential across a significant portion of the available phase space. However, we must stress that this is merely an informed projection, intended to underscore the importance of striving for the optimal design of future collider detectors and advancing Monte Carlo tool development to reduce modelling uncertainties.

## 5 Conclusions

Studying particle correlations in high-energy collider experiments provides crucial insights into the behavior of matter under extreme conditions, reminiscent of the early universe before quarks and gluons combined into hadrons. This method can serve as a complementary tool to traditional searches, offering the potential to detect new phenomena, including physics BSM, as proposed in Refs. [12, 13] and explored in this work.

Inspired by experimental findings of unusual angular correlation patterns in hadronic collisions, we investigated the potential for detecting hidden sectors at future  $e^+e^-$  colliders through two-particle angular correlation studies at the detector level. Our focus was on a QCD-like HV model, which includes  $v$ -quarks and  $v$ -gluons interacting with the SM via communicators with masses typically below 1 TeV. The analysis concentrated on  $D_v\bar{D}_v$  pair production at  $\sqrt{s} = 250 \text{ GeV}$ , around the expected mass of the lightest communicator in this scenario, with a brief extension to higher energies (up to 1 TeV), where we observed similarly encouraging prospects [8].

In summary, the results demonstrate that two-particle azimuthal correlations at a future  $e^+e^-$  Higgs factory could be an effective tool for uncovering new physics, assuming it is within the accessible kinematic range. Although this study focused on a specific HV model, other hidden sectors would likely produce comparable signatures. Additionally, we cannot rule out the possibility that collective effects, unrelated to BSM physics, could contribute to the observed correlations. These correlation-based approaches, which detect diffuse signals distributed across numerous final-state particles, should be considered complementary to standard methods, thereby increasing the likelihood of discovering new phenomena at future collider experiments.

## Acknowledgments

The author acknowledges financial support from the MCIN with funding from the European Union NextGenerationEU and from GV via the Programa de Planes Complementarios de I+D+i (PRTR 2022) Project *Si4HiggsFactories*, reference ASFAE/2022/015. In addition, the author acknowledges support from the European Union / FEDER via the grant PID2021-122134NB-C21.

## References

- [1] M.J. Strassler, K.M. Zurek, Echoes of a hidden valley at hadron colliders, *Phys. Lett. B* **651**, 374 (2007), [hep-ph/0604261](https://arxiv.org/abs/hep-ph/0604261). [10.1016/j.physletb.2007.06.055](https://doi.org/10.1016/j.physletb.2007.06.055)
- [2] T. Sjöstrand, S. Ask, J.R. Christiansen, R. Corke, N. Desai, P. Ilten, S. Mrenna, S. Prestel, C.O. Rasmussen, P.Z. Skands, An introduction to PYTHIA 8.2, *Comput. Phys. Commun.* **191**, 159 (2015), [1410.3012](https://arxiv.org/abs/1410.3012). [10.1016/j.cpc.2015.01.024](https://doi.org/10.1016/j.cpc.2015.01.024)
- [3] M. Berggren, SGV 3.0 – a fast detector simulation (2012), [1203.0217](https://arxiv.org/abs/1203.0217).
- [4] H. Abramowicz et al. (ILD Concept Group), International Large Detector: Interim Design Report (2020), [2003.01116](https://arxiv.org/abs/2003.01116).
- [5] T. Behnke et al., The International Linear Collider Technical Design Report - Volume 1: Executive Summary, *arXiv e-prints* (2013), [1306.6327](https://arxiv.org/abs/1306.6327). [10.48550/arXiv.1306.6327](https://doi.org/10.48550/arXiv.1306.6327)
- [6] E. Musumeci, R. Perez-Ramos, A. Irles, I. Corredoira, V.A. Mitsou, E. Sarkisyan-Grinbaum, M.A. Sanchis-Lozano, Two-particle angular correlations in the search for new physics at future  $e^+e^-$  colliders, in *International Workshop on Future Linear Colliders* (2023), [2307.14734](https://arxiv.org/abs/2307.14734)
- [7] A. Irles, J.P. Márquez, R. Pöschl, F. Richard, A. Saibel, H. Yamamoto, N. Yamatsu, Probing gauge-Higgs unification models at the ILC with quark–antiquark forward–backward asymmetry at center-of-mass energies above the Z mass, *Eur. Phys. J. C* **84**, 537 (2024), [2403.09144](https://arxiv.org/abs/2403.09144). [10.1140/epjc/s10052-024-12918-z](https://doi.org/10.1140/epjc/s10052-024-12918-z)
- [8] E. Musumeci, A. Irles, R. Perez-Ramos, I. Corredoira, E. Sarkisyan-Grinbaum, V.A. Mitsou, M.A. Sanchis-Lozano, Exploring hidden sectors with two-particle angular correlations at future  $e^+e^-$  colliders (2023), [2312.06526](https://arxiv.org/abs/2312.06526).
- [9] P. Bambade et al., The International Linear Collider: A Global Project (2019), [1903.01629](https://arxiv.org/abs/1903.01629).
- [10] M. Bahr et al., Herwig++ Physics and Manual, *Eur. Phys. J. C* **58**, 639 (2008), [0803.0883](https://arxiv.org/abs/0803.0883). [10.1140/epjc/s10052-008-0798-9](https://doi.org/10.1140/epjc/s10052-008-0798-9)
- [11] J. Bellm et al., Herwig 7.0/Herwig++ 3.0 release note, *Eur. Phys. J. C* **76**, 196 (2016), [1512.01178](https://arxiv.org/abs/1512.01178). [10.1140/epjc/s10052-016-4018-8](https://doi.org/10.1140/epjc/s10052-016-4018-8)

- [12] M.A. Sanchis-Lozano, Prospects of searching for (un)particles from Hidden Sectors using rapidity correlations in multiparticle production at the LHC, *Int. J. Mod. Phys. A* **24**, 4529 (2009), [0812.2397](https://doi.org/10.1142/S0217751X09045820). [10.1142/S0217751X09045820](https://doi.org/10.1142/S0217751X09045820)
- [13] M.A. Sanchis-Lozano, E.K. Sarkisyan-Grinbaum, Searching for new physics with three-particle correlations in  $pp$  collisions at the LHC, *Phys. Lett. B* **781**, 505 (2018), [1802.06703](https://doi.org/10.1016/j.physletb.2018.04.033). [10.1016/j.physletb.2018.04.033](https://doi.org/10.1016/j.physletb.2018.04.033)